CHINESE OPTICS LETTERS

Vol. 23, No. 10 | October 2025

Propagation of Airy beams on an incoherent background through atmospheric turbulence

Morteza Hajati[1], Zhiheng Xu (徐志恒)[2], Tianyu Cao (曹添宇)[3], and Sergey A. Ponomarenko[1,4*]

[1] Department of Electrical and Computer Engineering, Dalhousie University, Halifax B3J 2X4, Canada

[2] School of Physics and Electronic Engineering, Jining University, Qufu 273155, China

[3] Shandong Provincial Engineering and Technical Center of Light Manipulation and Shandong Provincial Key Laboratory of Optics and Photonic Devices, School of Physics and Electronics, Shandong Normal University, Jinan 250014, China

[4] Department of Physics and Atmospheric Science, Dalhousie University, Halifax B3H 4R2, Canada

*Corresponding author: serpo@dal.ca

Received April 28, 2025 | Accepted May 30, 2025 | Posted Online September 8, 2025

We numerically demonstrate that a recently discovered and experimentally realized class of partially coherent Airy beams atop an incoherent background remains robust during propagation through a statistically homogeneous isotropic random medium, such as the turbulent atmosphere. We show that these Airy beams on an incoherent background, which are propagation-invariant in free space, can mitigate turbulence-induced intensity fluctuations under both weak and strong turbulence conditions. We utilize a pseudo-modal decomposition to numerically model the intensity distribution of these beams, with results that agree well with analytical predictions. Additionally, we show that, compared to their fully coherent counterparts, Airy beams on an incoherent background better preserve their spatial structure under turbulence, making them promising candidates for modern optical communication through atmospheric turbulence.

Keywords: structured random light; Airy beam; atmospheric turbulence; diffraction-free beam; free-space optical communication.

DOI: 10.3788/COL202523.100003

1. Introduction

The exploration of structured random light beams has been central to optical coherence theory[1]. Such beams have attracted much interest since Collett and Wolf predicted that they can generate optical fields as directional as those produced by lasers[2]. To date, however, most of the work on structured random light has been focused on statistically uniform fields, possessing Schell-model correlations[3]. While Schell-model correlated beams had initially held much promise for free space optical communications[4–6], it has become clear lately that the spatial correlation structure of their fields makes them vulnerable to distortions caused by atmospheric turbulence in the strong fluctuation regime, or over long propagation distances in the turbulent atmosphere[7,8]. As is well documented[9,10] the loss of a well-defined spatial intensity distribution of light at the source is one of the most devastating effects of atmospheric turbulence. One approach to alleviate the adverse effects of turbulence on the spatial intensity distribution of the field of a random beam propagating through atmospheric turbulence is to structure the field correlations of the beam in the transverse plane to be non-uniform. The first such beam model was introduced and the source correlations were obtained in a closed form in Ref. [11]. This theoretical work was followed by the experimental realization of non-uniformly correlated beams composed of two[12] and multiple uncorrelated modes[13], as well as by further theoretical[14–18] and experimental[19–21] work on structuring non-uniformly correlated beams. For comprehensive reviews of non-uniformly correlated beams and surface electromagnetic waves, see Refs. [22,23].

Further, it has been demonstrated theoretically[14] and experimentally[19,24] that propagation invariant random wave packets in free space necessarily feature non-uniform correlations as they manifest themselves as bumps/dips residing atop a statistically uniform background. One of the most attractive features of such diffraction-free beams is their capacity to remain structurally stable on propagation through a statistically homogeneous isotropic random medium, such as the turbulent atmosphere[7].

Recently, coherent diffraction-free Airy wave packets have attracted much attention in both quantum mechanics[25] and optics[26,27] due to their unique properties[28]. Airy beams on incoherent background (ABIB) have also been discovered and experimentally realized[29,30]. Specifically, we have shown elsewhere[29] how ABIB can be structured such that every ABIB family member is represented by an Airy bump situated on a Gaussian-correlated homogeneous background. As far as free-space optical communications are concerned, an interesting question then arises: is the spatial structure of ABIB robust on propagation through the turbulent atmosphere, and if so, how does the turbulence strength affect their degradation?

In this Letter, we show that Airy beams on incoherent background, which defy diffraction in free space, do manifest robust behavior when propagating through any statistically homogeneous and isotropic random medium such as the turbulent atmosphere. More precisely, our numerical simulations indicate that, compared to a generic coherent Airy beam, ABIBs are highly effective in suppressing the adverse effects of both weak and strong turbulence. We employ pseudo-mode decomposition of the cross-spectral density of the beam to numerically generate the ABIB intensity distribution. Our numerical modeling of the source is in good agreement with the analytical theory and hence can be reliably used in subsequent numerical simulations of ABIB propagation through turbulence. The self-healing nature of ABIB sources in random media suggests their potential for optical communications and information transfer through the turbulent atmosphere.

2. Analytical Theory: A Review

Let us start by briefly reviewing how the Airy beam on an incoherent background source can be devised. We demonstrated in Ref. [29] that an ABIB can be generated using a continuum of plane wave modes with the amplitude $\mathcal{A}(\mathbf{k},\mathbf{r})$. Each plane wave contribution to the overall source intensity is weighed with a non-negative Gaussian function $p(\mathbf{k})$. We can then represent the cross-spectral density of the two-dimensional (2D) ABIB as[31]

$$W(\mathbf{r}_1,\mathbf{r}_2)=\int \mathrm{d}\mathbf{k}p(\mathbf{k})\mathcal{A}^*(\mathbf{k},\mathbf{r}_1)\mathcal{A}(\mathbf{k},\mathbf{r}_2), \tag{1}$$

where

$$p(\mathbf{k})=\prod_{j=x,y}\frac{\sigma_{cj}}{\sqrt{2\pi}}\exp\left(-\frac{k_j^2\sigma_{cj}^2}{2}\right), \tag{2}$$

and

$$\mathcal{A}(\mathbf{k},\mathbf{r})\propto\cos\left(\frac{1}{6}\sum_{j=x,y}\sigma_{Ij}^3k_j^3+\frac{1}{2}\mathbf{k}\cdot\mathbf{r}\right). \tag{3}$$

The background coherence width, σ_{cj}, and the bump intensity width, σ_{Ij}, are introduced along the Cartesian coordinate axes $j=x,y$. Additionally, $\mathbf{r}=(x,y)$ and $\mathbf{k}=(k_x,k_y)$ denote the 2D position vector in the source plane and the corresponding wave-vector in the reciprocal space, respectively.

Following the approach advanced in[29], we can express the 2D cross-spectral density of an Airy beam on an incoherent background in dimensionless variables as

$$W_{\mathrm{A}}(\mathbf{R}_-,\mathbf{R}_+)=W_{\mathrm{bg}}(\mathbf{R}_-)+W_{\mathrm{bp}}(\mathbf{R}_+), \tag{4}$$

with

$$W_{\mathrm{bg}}(\mathbf{R}_-)\propto\exp\left(-\frac{X_-^2}{8\xi_{cx}}-\frac{Y_-^2}{8\xi_{cy}}\right), \tag{5}$$

and

$$W_{\mathrm{bp}}(\mathbf{R}_+)\propto P_{2D}\exp\left(\frac{\xi_{cx}^3+\xi_{cy}^3}{12}\right)\exp\left(\frac{\xi_{cx}X_+}{2}\right)\exp\left(\frac{\xi_{cy}Y_+}{2}\right)\times\mathrm{Ai}\left(X_++\frac{\xi_{cx}^2}{4}\right)\mathrm{Ai}\left(Y_++\frac{\xi_{cy}^2}{4}\right). \tag{6}$$

Here, $W_{\mathrm{bg}}(\mathbf{R}_-)$ denotes the cross-spectral density of a statistically homogeneous background with Gaussian correlations and $W_{\mathrm{bp}}(\mathbf{R}_+)$ represents an Airy bump atop the background. We introduce dimensionless variables $X_\pm$ and $Y_\pm$ as the center-of-mass and difference coordinates. Finally, the 2D ABIB source intensity $I_A(\mathbf{R})=W_A(\mathbf{R},\mathbf{R})$ is obtained from Eq. (4) by setting $\mathbf{R}_-=(X_-,Y_-)=(0,0)$ and $\mathbf{R}_+=(X_+,Y_+)=(X,Y)$, leading to

$$I_{\mathrm{A}}(\mathbf{R})\propto 1+P_{\mathrm{2D}}\exp\left(\frac{\xi_{cx}^3+\xi_{cy}^3}{12}\right)\exp\left(\frac{\xi_{cx}X}{2}\right)\exp\left(\frac{\xi_{cy}Y}{2}\right)\times\mathrm{Ai}\left(X+\frac{\xi_{cx}^2}{4}\right)\mathrm{Ai}\left(Y+\frac{\xi_{cy}^2}{4}\right), \tag{7}$$

where $\xi_{cj}=(\sigma_{cj}/\sigma_{Ij})^2$ is a correlation parameter and $P_{\mathrm{2D}}=2\pi\sqrt{\xi_{cx}\xi_{cy}}$ is the total power (in dimensionless units) of the 2D Airy bump relative to the background.

The pseudo-mode decomposition method is a reliable technique to numerically generate the 2D ABIB cross-spectral density represented in the previous section. This approach is particularly effective for the numerical and experimental realization of structured random sources, as it significantly reduces the problem's dimensionality and computational complexity.

Using this method, the evolution of the source cross-spectral density is revealed through an appropriate superposition of uncorrelated pseudo-modes. There are a number of alternative variants of the pseudo-mode decomposition that have been proposed to date[32–36]. One common approach to discretize the source cross-spectral density is to sample the non-negative Gaussian weighted function $p(\mathbf{k}_{mn})$ and the modes such that

$$W(\mathbf{r}_1,\mathbf{r}_2)=\sum_{m,n}p(\mathbf{k}_{mn})\mathcal{A}^*(\mathbf{k}_{mn},\mathbf{r}_1)\mathcal{A}(\mathbf{k}_{mn},\mathbf{r}_2), \tag{8}$$

where m and n are two integers that represent mode indices. In the 2D representation of the cross-spectral density, $\mathbf{k}_{mn}=(k_{mx},k_{ny})$ is defined as a discrete vector in the transverse plane. Theoretically, reconstructing the ABIB source requires an infinite number of pseudo-modes. In practice, however, the summation on the right-hand side of Eq. (8) can be truncated to achieve any desired level of accuracy.

3. Results and Discussion

In this section, we first compare the numerical realization of the ABIB source with exact analytical results to validate the former. We then introduce a random phase screen (RPS) approach for numerical simulation of ABIB propagation through a random medium. Finally, we employ the RPS method to study the average intensity evolution of the ABIB during propagation through the turbulent atmosphere and compare it with that of a generic coherent Airy beam.

3.1. Comparison of numerically generated ABIBs with exact analytics

To validate the numerical pseudo-mode representation discussed earlier, we compare the intensity profiles of the generated ABIB source with the corresponding analytical expressions. Figure 1 illustrates the results for different values of the correlation parameter: 0.1 (left panels), 0.3 (middle panels), and 0.5 (right panels). The top row shows the analytically generated 2D intensity source profiles of ABIBs derived from Eq. (7), while the middle row presents the numerical reconstructions of these profiles based on the pseudo-mode representation in Eq. (8). To enable quantitative comparison, corresponding 1D cross-sections are also generated, with theoretical and numerical results shown as the solid and dashed curves, respectively. As shown, the numerically reconstructed profiles exhibit excellent agreement with analytical predictions, confirming the accuracy and reliability of the pseudo-mode representation approach.

It is important to note that the number of pseudo-modes needed for accurate ABIB source reconstruction depends on the correlation parameter, with lower values significantly increasing the required number of pseudo-modes and, consequently, the computational cost. Therefore, the correlation parameter must be carefully chosen to balance numerical accuracy and computational efficiency. For a faithful reconstruction of the ABIB source in 2D simulations, we find that 240^2, 100^2, and 64^2 pseudo-modes are required to accurately reproduce spatial intensity distributions for correlation parameters of 0.1, 0.3, and 0.5, respectively.

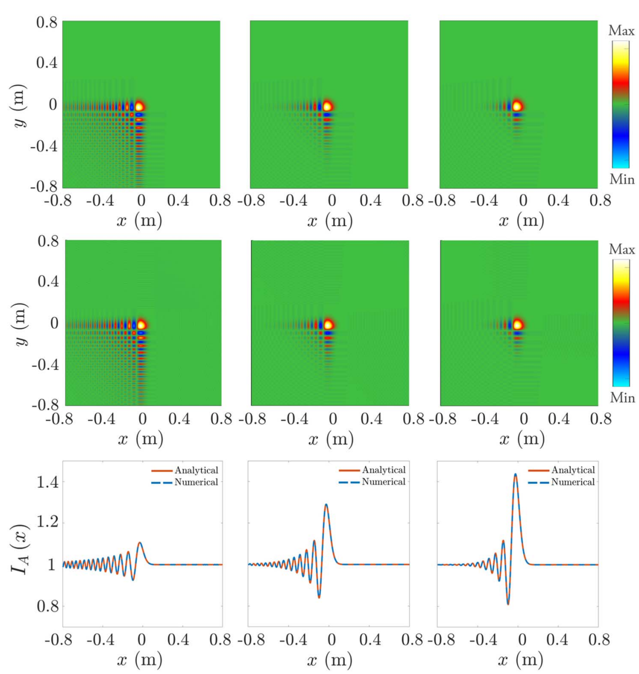

Fig. 1. (Top row) Theoretically generated 2D intensity source profiles of ABIBs derived from Eq. (7). (Middle row) Numerically reconstructed 2D intensity source profiles of ABIBs derived from Eq. (8). (Bottom row) Comparison of the corresponding 1D cross-sections of the ABIB source profiles obtained analytically as solid curves and numerically as dashed curves. The correlation parameter is set to 0.1 (left), 0.3 (middle), and 0.5 (right).

3.2. Random phase screen method

The random phase screen method is a well-established computational technique for modeling the transmission of electromagnetic beams through an extended random medium[37]. The RPS approach amounts to modeling the extended random medium as a series of thin phase screens placed along the transmission path at equal intervals such that each screen is perpendicular to the direction of beam propagation. We illustrate in Fig. 2 the schematics of the RPS method for optical beam propagation through atmospheric turbulence. The propagation distance D is divided into N segments of equal length such that $d = D/N$.

Within the RPS framework, the optical field evolution is approximated as follows. The evolution of a beam in a random medium is governed by the interplay of two factors: free-space diffraction and atmospheric turbulence. The propagation region is composed of turbulence-free subregions between adjacent phase screens, where amplitude variations are primarily accumulated due to diffraction over the entire propagation length. At the same time, turbulence effects are accounted for as the beam field is transmitted through a series of thin diffraction-free phase screen regions, whereby phase fluctuations are mainly accumulated due to the presence of random medium inhomogeneities. Thus, both the amplitude and phase of the beam experience distortions during the entire transmission process.

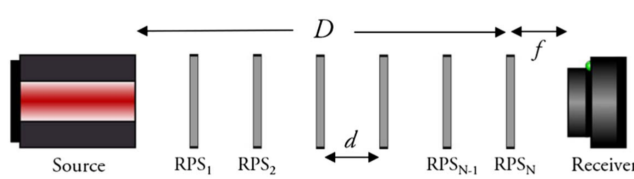

Fig. 2. Schematics of beam propagation through atmospheric turbulence. RPS_1–RPS_N represent the first and last phase screens and N denotes the number of phase screens employed in the simulations.

To numerically simulate beam propagation through the turbulent atmosphere using the RPS method, we adopt the modified von Karman spectrum model[37] to describe the refractive index fluctuations within the statistically homogeneous and isotropic turbulent atmosphere. In this context, the power spectrum of the phase screen Φ_θ and the power spectrum of the refractive index fluctuations Φ_n are related via $\Phi_\theta = 2\pi d k^2 \Phi_n$. It follows that the spectrum of the refractive index fluctuations can be expressed as

$$\Phi_n(\kappa) = 0.033 C_n^2 \frac{\exp(-\kappa^2/\kappa_m^2)}{(\kappa^2 + \kappa_0^2)^{11/6}}, \quad 0 \le \kappa < \infty, \tag{9}$$

where $\kappa_m = 5.92/l_0$ and $\kappa_0 = 2\pi/L_0$. Here, $l_0 = 1$ mm is an inner scale of the turbulence, $L_0 = 1$ m is an outer scale of the turbulence, and C_n^2 is a structure constant describing the strength of refractive index fluctuations induced by turbulence.

The remaining parameters for the ABIB source and random medium are as follows. We fix the carrier wavelength at $\lambda = 632.8\,\mathrm{nm}$. The correlation parameter is set to 0.3, corresponding to a background coherence width of 16.4 mm and an Airy bump intensity width of 30 mm. In the weak turbulence regime, the structure constant is chosen as $C_n^2 = 1 \times 10^{-17}\,\mathrm{m}^{-2/3}$. The number of random phase screens employed in the simulations is $N = 6$, and the distance between adjacent screens is adopted to be $d = 400\,\mathrm{m}$, extending the propagation range up to 2000 m. Under strong turbulence conditions, the structure constant is chosen as $C_n^2 = 1 \times 10^{-13}\,\mathrm{m}^{-2/3}$. The simulations use $N = 13$ random phase screens, with the distance between adjacent screens set to $d = 25\,\mathrm{m}$, allowing the propagation range to extend up to 300 m. The number of phase screens and the selected distance between them are chosen to satisfy the Rytov coefficient requirements[38].

3.3. Weak and strong turbulence simulations

In this section, we examine the average intensity evolution of ABIBs under weak and strong turbulence conditions. For comparison, we consider a coherent Airy beam with a source-plane field envelope given by $U(x/x_0, y/y_0) = \mathrm{Ai}(x/x_0)\exp(ax/x_0)\,\mathrm{Ai}(y/y_0)\exp(ay/y_0)$,[26] where x and y are the coordinates in the source plane and x_0 and y_0 are their corresponding transverse scales. The cut-off length is denoted by a.

To ensure a fair comparison, the ABIB and the coherent Airy beam sources must have identical widths of their main lobes and roughly the same number of secondary lobes. For an ABIB with the correlation parameter of 0.3, these conditions are satisfied by setting $x_0 = y_0 = 30\,\mathrm{mm}$ and $a = 0.15$ for the coherent Airy beam source. In Fig. 3, we explore the average intensity evolution of both beams as they propagate in the weakly turbulent atmosphere. The results show that the average intensity profiles of ABIBs remain nearly invariant over propagation distances of up to 2000 m, demonstrating their remarkable resilience to atmospheric turbulence and the ability to maintain their spatial structure over fairly long distances as long as turbulence is relatively weak (top panels). In contrast, the coherent Airy beam loses most of its side lobes, retaining only a short tail, which indicates significant degradation of its spatial structure due to turbulence effects (bottom panels). This deterioration is expected to intensify with the propagation distance, further diminishing the distinct features of coherent Airy beams.

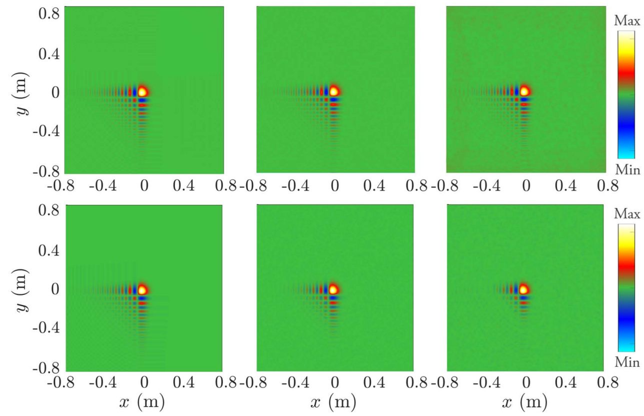

Fig. 3. Average intensity distributions of the ABIB (top panels) and the coherent Airy beam (bottom panels) propagating in a stretch of the weakly turbulent atmosphere over the thickness set to 0 (left), 1200 m (middle), and 2000 m (right). The structure constant is chosen as $C_n^2 = 1 \times 10^{-17}\,\mathrm{m}^{-2/3}$.

In Fig. 4, we present the average intensity profiles of an ABIB and its coherent counterpart under strong turbulence conditions. We can infer from the figure that the ABIB experiences only slight degradation in its tail while preserving its main lobe, thereby maintaining its structural integrity over propagation distances of up to 300 m (top panels). In contrast, the coherent Airy beam not only loses most of its oscillatory tail, just as it does in the weakly turbulent regime, but also experiences noticeable distortion of its main lobe due to deleterious effects of strong turbulence (bottom panels).

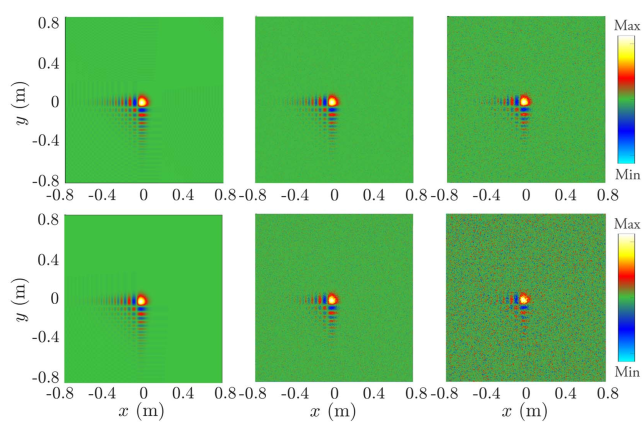

Fig. 4. Average intensity distributions of the ABIB (top panels) and the coherent Airy beam (bottom panels) propagating in the strongly turbulent atmosphere over the propagation distance set to 0 (left), 150 m (middle), and 300 m (right). The structure constant is chosen as $C_n^2 = 1 \times 10^{-13}\,\mathrm{m}^{-2/3}$.

Although the coherent Airy beam is an accelerating beam, the simulations in Figs. 3 and 4 do not show its acceleration. This is because the effective acceleration length of the beam exceeds the range of propagation distances considered here. This circumstance is due to the fact that we have adjusted the source plane scale of the coherent Airy beam to match that of the ABIB leading to negligible acceleration effects over the computational window adopted in this work.

4. Conclusion

We have numerically demonstrated that Airy beams on incoherent background maintain a robust average intensity profile and outperform conventional coherent Airy beams in preserving their well-defined spatial structure on propagation in the turbulent atmosphere. We can attribute the robustness of ABIBs against atmospheric turbulence to two key factors. First, the ABIBs are composed of a multitude of uncorrelated modes with random phases, making them insensitive to phase fluctuations caused by atmospheric turbulence. Second, the Airy shape of their main lobe does endow them with intrinsic self-healing properties that have been experimentally demonstrated[30]. The structural stability of ABIBs in atmospheric turbulence makes these beams attractive candidates for free-space optics, information transfer, and imaging in random media.

Acknowledgements

This work was supported by the Natural Sciences and Engineering Research Council of Canada (No. RGPIN-2025-04064).

References

1. L. Mandel and E. Wolf, *Optical Coherence and Quantum Optics* (Cambridge University, 1995).
2. E. Collett and E. Wolf, "Is complete spatial coherence necessary for the generation of highly directional light beams?" Opt. Lett. **2**, 27 (1978).
3. Y. Cai, Y. Chen, J. Yu, *et al.*, "Generation of partially coherent beams," Prog. Opt. **62**, 157 (2017).
4. S. A. Ponomarenko, J.-J. Greffet, and E. Wolf, "The diffusion of partially coherent beams in turbulent media," Opt. Commun. **208**, 1 (2002).
5. G. Gbur and E. Wolf, "Spreading of partially coherent beams in random media," J. Opt. Soc. Am. A **19**, 1592 (2002).
6. X. Liu, J. Yu, Y. Cai, *et al.*, "Propagation of optical coherence lattices in the turbulent atmosphere," Opt. Lett. **41**, 4182 (2016).
7. Z. Xu, X. Liu, Y. Cai, *et al.*, "Structurally stable beams in the turbulent atmosphere: dark and antidark beams on incoherent background," J. Opt. Soc. Am. A **39**, C51 (2022).
8. S. A. Ponomarenko, "Classical entanglement of twisted random light propagating through atmospheric turbulence," J. Opt. Soc. Am. A **39**, 2224 (2022).
9. G. Gbur, "Partially coherent beam propagation in atmospheric turbulence," J. Opt. Soc. Am. A **31**, 2038 (2014).
10. F. Wang, X. Liu, and Y. Cai, "Propagation of partially coherent beam in turbulent atmosphere: a review (invited review)," Prog. Electromagn. Res. **150**, 123 (2015).
11. S. A. Ponomarenko, "A class of partially coherent beams carrying optical vortices," J. Opt. Soc. Am. A **18**, 150 (2001).
12. G. V. Bogatyryova, C. V. Felde, P. V. Polyanskii, *et al.*, "Partially coherent vortex beams with a separable phase," Opt. Lett. **28**, 878 (2003).
13. X. Chen, J. Li, S. M. H. Rafsanjani, *et al.*, "Synthesis of Im-Bessel correlated beams via coherent modes," Opt. Lett. **43**, 3590 (2018).
14. S. A. Ponomarenko, W. Huang, and M. Cada, "Dark and antidark diffraction-free beams," Opt. Lett. **32**, 2508 (2007).
15. R. Borghi, F. Gori, and S. A. Ponomarenko, "On a class of electromagnetic diffraction-free beams," J. Opt. Soc. Am. A **26**, 2275 (2009).
16. H. Lajunen and T. Saastamoinen, "Propagation characteristics of partially coherent beams with spatially varying correlations," Opt. Lett. **36**, 4104 (2011).
17. J. Yu, F. Wang, L. Liu, *et al.*, "Propagation properties of Hermite non-uniformly correlated beams in turbulence," Opt. Express **26**, 16333 (2018).
18. M. W. Hyde and S. Avramov-Zamurovic, "Generating dark and antidark beams using the genuine cross-spectral density function criterion," J. Opt. Soc. Am. A **36**, 1058 (2019).
19. X. Zhu, F. Wang, C. Zhao, *et al.*, "Experimental realization of dark and anti-dark diffraction-free beams," Opt. Lett. **44**, 2260 (2019).
20. Y. Shen, H. Sun, D. Peng, *et al.*, "Optical image reconstruction in 4f imaging system: Role of spatial coherence structure engineering," Appl. Phys. Lett. **118**, 181102 (2021).
21. D. Peng, Z. Huang, Y. Liu, *et al.*, "Optical coherence encryption with structured random light," PhotoniX **2**, 6 (2021).
22. Y. Cai, Y. Chen, and F. Wang, "Generation and propagation of partially coherent beams with nonconventional correlation functions: a review," J. Opt. Soc. Am. A **31**, 2083 (2014).
23. Y. Chen, A. Norrman, S. A. Ponomarenko, *et al.*, "Optical coherence and electromagnetic surface waves," Prog. Opt. **65**, 105 (2020).
24. M. Yessenov, B. Bhaduri, H. E. Kondakci, *et al.*, "Non-diffracting broadband incoherent space-time fields," Optica **6**, 598 (2019).
25. M. V. Berry and N. L. Balazs, "Nonspreading wave packets," Am. J. Phys. **47**, 264 (1979).
26. G. A. Siviloglou and D. N. Christodoulides, "Accelerating finite energy Airy beams," Opt. Lett. **32**, 979 (2007).
27. G. A. Siviloglou, J. Broky, A. Dogariu, *et al.*, "Observation of accelerating Airy beams," Phys. Rev. Lett. **99**, 213901 (2007).
28. J. Broky, G. A. Siviloglou, A. Dogariu, *et al.*, "Self-healing properties of optical Airy beams," Opt. Express **16**, 12880 (2008).
29. M. Hajati, V. Sieben, and S. A. Ponomarenko, "Airy beams on incoherent background," Opt. Lett. **46**, 3961 (2021).
30. Q. Chen, M. Hajati, X. Liu, *et al.*, "Experimental realization of Airy beams on incoherent background," Opt. Laser Technol. **169**, 110020 (2024).
31. F. Gori and M. Santarsiero, "Devising genuine spatial correlation functions," Opt. Lett. **32**, 3531 (2007).
32. Y. Gu and G. Gbur, "Scintillation of pseudo-Bessel correlated beams in atmospheric turbulence," J. Opt. Soc. Am. A **27**, 2621 (2010).
33. S. A. Ponomarenko, "Complex Gaussian representation of statistical pulses," Opt. Express **19**, 17086 (2011).
34. S. Zhu, P. Li, Z. Li, *et al.*, "Generating non-uniformly correlated twisted sources," Opt. Lett. **46**, 5100 (2021).
35. F. Wang, H. Lv, Y. Chen, *et al.*, "Three modal decompositions of Gaussian Schell-model sources: comparative analysis," Opt. Express **29**, 29676 (2021).
36. X. Liu, Q. Chen, J. Zeng, *et al.*, "Measurement of optical coherence structures of random optical fields using generalized Arago spot experiment," Opto-Electron. Sci. **2**, 220024 (2023).
37. L. C. Andrews and R. L. Phillips, *Laser Beam Propagation in Turbulent Atmosphere*, 2nd ed. (SPIE, 2005).
38. J. D. Schmidt, *Numerical Simulation of Optical Wave Propagation: With Examples in MATLAB* (SPIE, 2010).